



Supplementary Information for

**Rapid reductions and millennial-scale variability in Nordic Seas sea ice cover during abrupt glacial climate changes**

Henrik Sadatzki\*, Niccolò Maffezzoli, Trond M. Dokken, Margit H. Simon, Sarah M. P. Berben, Kirsten Fahl, Helle A. Kjær, Andrea Spolaor, Ruediger Stein, Paul Vallenga, Bo M. Vinther, Eystein Jansen

\* Corresponding author: Henrik Sadatzki  
**Email:** [henrik.sadatzki@awi.de](mailto:henrik.sadatzki@awi.de)

**This PDF file includes:**

SI Text  
Figures S1 to S4  
Tables S1 to S2  
SI References

## Supplementary Information Text

### Materials and Methods

#### Chronology

Age models of cores MD95-2010 and MD99-2284 are based on the near-surface temperature record (1) and cryptotephra layers (2) from core MD99-2284, in conjunction with anhysteretic remanent magnetization (ARM) records of MD99-2284 (1) and MD95-2010 (3, 4). In core MD99-2284, near-surface temperature estimates based on planktic foraminifera census counts reveal pronounced temperature overshoots of 2–3°C, whose abrupt onsets parallel the mid points of ARM increases (1, 5). Recently published cryptotephra evidence from core MD99-2284 shows that the rapid 2–3°C warming transitions in the Southern Norwegian Sea were coeval with the abrupt D-O warming transitions over Greenland (2). In particular, four distinct cryptotephra layers were identified before and after the GS6-GI5 transition as well as during GI6 and GI8 in both core MD99-2284 and the NGRIP ice core with a consistent geochemistry reflecting a Kverkfjöll, Katla, Kverkfjöll and Grímsvötn volcanic source, respectively (2) (Fig. S2). Accordingly, the age model of MD99-2284 is based on alignment of near-surface temperature signals and D-O climate transitions in the NGRIP  $\delta^{18}\text{O}$  record, independently verified and constrained by four cryptotephra isochrons (2). This age model also results in a positive and in-phase correlation between ARM in core MD99-2284 with NGRIP  $\delta^{18}\text{O}$  (Fig. S2), generally verifying an ARM-based tuning approach used in previous studies (1, 5).

The ARM record of MD95-2010 reveals a variability that is very consistent with that in core MD99-2284 and resembles the D-O climate variability in NGRIP  $\delta^{18}\text{O}$  (Fig. S2). It has been suggested that variations in sedimentary ARM are related to changes in deep/bottom current speed and associated effects on the efficiency of magnetic particle transport from the Greenland-Scotland ridge area into the Nordic Seas and North Atlantic, co-varying with millennial-scale D-O climate changes during the last glacial (3, 6). In agreement with a weakened AMOC (7, 8), we tie intervals of decreased ARM in MD95-2010, reflecting a reduced deep current activity, to intervals of decreased ARM in MD99-2284 and cold GS in the NGRIP  $\delta^{18}\text{O}$  record (Fig. S2). Vice versa, we tie intervals of an increased ARM in MD95-2010, reflecting enhanced deep current activity, to intervals of increased ARM in MD99-2284 and the warm GI in the NGRIP  $\delta^{18}\text{O}$  record. Thereby, we slightly revised the original age model of core MD95-2010 by ref. 4.

The final age models are based on 13 tie points in MD95-2010 (Table S1) and 13 tie points in MD99-2284 (Table S2; adopting the tie points from ref. 2), as well as linear interpolation between them. Resulting sedimentation rates average ~16 cm/ka in MD95-2010 and ~155 cm/ka in MD99-2284 for the interval 32–41 ka and reveal a consistent pattern in both cores with increased sediment deposition during GI (Table S1, Table S2). These age models are consistent with those recently presented for both cores by ref. 9, but show a better alignment for GI9 and GI10 in MD95-2010 (Fig. S2).

The chronology of the RECAP ice core is based on alignment of the RECAP dust record to the NGRIP  $\delta^{18}\text{O}$  (10) (Fig. S2). A few minor offsets between the RECAP dust and NGRIP  $\delta^{18}\text{O}$  and dust may explain why the lowered  $\text{Br}_{\text{enr}}$  value of GI9 lies shortly after the interstadial (Fig. 3). Nevertheless, especially the cold-to-warm GS-GI transitions are precisely aligned.

Finally, the depth scales of sediment cores MD95-2010 and MD99-2284 and the RECAP ice core are all transferred to the GICC05 b2k time scale (11). Hence, temporal variations in our sediment core-based and ice core-based sea ice records investigated in this study are robust and can directly be compared with each other.

### **Biomarker analysis of marine sediments**

Biomarker analyses of 75 samples from core MD95-2010 (between 700 cm and 840 cm core depth) and 41 samples from GS15-198, GS16-204 and FRAM2014/15 multicore-tops (0–1 cm core depth each) were performed at the Alfred Wegener Institute, Bremerhaven, Germany, using the methodology outlined here. Analyses and the slightly different extraction method applied on samples from core MD99-2284 are detailed in ref. 5. Highly-branched isoprenoids (HBI) and sterols and were extracted from ~5 g of freeze-dried and homogenized sediment by ultrasonication and using dichloromethane:methanol (2:1, v/v) as solvent ( $3 \times 30$  ml), after addition of internal standards 7-hexylnonadecane (7-HND, 0.076  $\mu\text{g}$ , for HBI quantification), 9-octylheptadec-8-ene (9-OHD, 0.1  $\mu\text{g}$ ), 5 $\alpha$ -androstan-3 $\beta$ -ol (androstanol, 11.5  $\mu\text{g}$ , for sterol quantification), and squalane (2.4  $\mu\text{g}$ ) to each sample. Extracts were separated into hydrocarbon and sterol fractions through open-column chromatography ( $\text{SiO}_2$ ) using 5 ml *n*-hexane and 9 ml ethylacetate:*n*-hexane (2:8, v/v), respectively. The sterol fraction was silylated with 200  $\mu\text{l}$  BSTFA (bis-trimethylsilyl-trifluoroacet-amide) (60°C, 2 h) for sterol analyses. As all samples were spiked before extraction with internal standards that are chemically similar to the biomarkers of interest, and HBI and sterol concentrations were shown to be comparable for extraction with accelerated solvent extractor or ultrasonication (12), we exclude a significant extraction bias of the differences in biomarker values between cores MD95-2010 and MD99-2284.

Biomarkers were analyzed by gas chromatography/mass spectrometry using an Agilent 7890B GC coupled to an Agilent 5977A mass selective detector (MSD) in selected ion monitoring mode for HBI, and an Agilent 6850 GC coupled with an Agilent 5975C VL MSD for sterols. HBI and sterol identification was based on comparison of GC retention times with those of reference compounds and published mass spectra for sterols (13, 14) and for IP<sub>25</sub> and HBI-III (15, 16). IP<sub>25</sub> and HBI-III were quantified using its molecular ions  $m/z$  350 and  $m/z$  346, respectively, in relation to the abundant fragment ion  $m/z$  266 of the internal standard 7-HND (for details see ref. 17). Brassicasterol (24-methylcholesta-5,22E-dien-3 $\beta$ -ol) was quantified as trimethylsilyl ether using its molecular ions  $m/z$  470 in relation to the molecular ion  $m/z$  348 of the internal standard androstanol. Biomarker concentrations were normalized to the total organic carbon (OC) content that was measured on ~100 mg of sediment from each sample used for biomarker analyses.

To generate semi-quantitative estimates of the past sea ice cover, we calculated the phytoplankton-IP<sub>25</sub> index established by ref. 18:

$$PIP_{25} = [IP_{25}] / ([IP_{25}] + ([\text{phytoplankton marker}] \times c)) \quad (1)$$

As phytoplankton marker we used brassicasterol (P<sub>B</sub>IP<sub>25</sub>) and HBI-III (P<sub>III</sub>IP<sub>25</sub>). The balance factor *c* corresponds to the ratio of mean IP<sub>25</sub> and mean phytoplankton concentration for MD95-2010 records (*c*=0.013 for P<sub>B</sub>IP<sub>25</sub>, *c*=0.68 for P<sub>III</sub>IP<sub>25</sub>). For GS15-198, GS16-204 and FRAM2014/15 core-tops presented in our study we estimate *c*=0.007 for P<sub>B</sub>IP<sub>25</sub> and *c*=2.0 for P<sub>III</sub>IP<sub>25</sub>. For the compilation of Arctic and sub-Arctic core-top P<sub>B</sub>IP<sub>25</sub> values shown in Figure 1 we used a uniform balance factor of *c*=0.023, following ref. 19.

### **Bromine and sodium analyses of RECAP ice core samples**

Bromine (Br) and sodium (Na) analyses were performed on RECAP ice core samples between 535.7 m and 537.35 m core depth, resulting in 50 data points between ~29 ka and 40 ka. The continuous sections of 0.55 m length each were cut and processed in 2015 at the Alfred Wegener Institute, Bremerhaven, Germany. Samples used for the analyses were obtained at the Center for Ice and Climate, Copenhagen, Denmark, by melting the 0.55 m ice sections at ~1 cm min<sup>-1</sup> in a standard Continuous Flow Analysis setup (20) and collecting the delivered water volume downstream the melt head in Polypropylene vials. Water samples were immediately refrozen and shipped to the Institute of Polar Science of the National Research Council of Italy, Venice, Italy, for analytical determination of Br and Na by Collision Reaction Cell-Inductively Coupled Plasma-Mass Spectrometry (CRC-ICP-MS). In addition to Br and Na, calcium was analyzed in the same ice core samples and used to calculate the sea salt Na (ssNa) contribution, since part of the total Na content (10–50%) may derive from dust, especially during GS (Fig. S4). Further details on the ssNa calculation are given in ref. 21.

Ice core bromine enrichment (Br<sub>enr</sub>) values were calculated based on the equation by ref. 21:

$$Br_{enr} = ([Br]/[ssNa])_{ice} / ([Br]/[Na])_{sw} \quad (2)$$

The ([Br]/[ssNa])<sub>ice</sub> is obtained from ice core samples and normalized by the seawater bromine-to-sodium mass ratio ([Br]/[Na])<sub>sw</sub>=0.0062 (22).

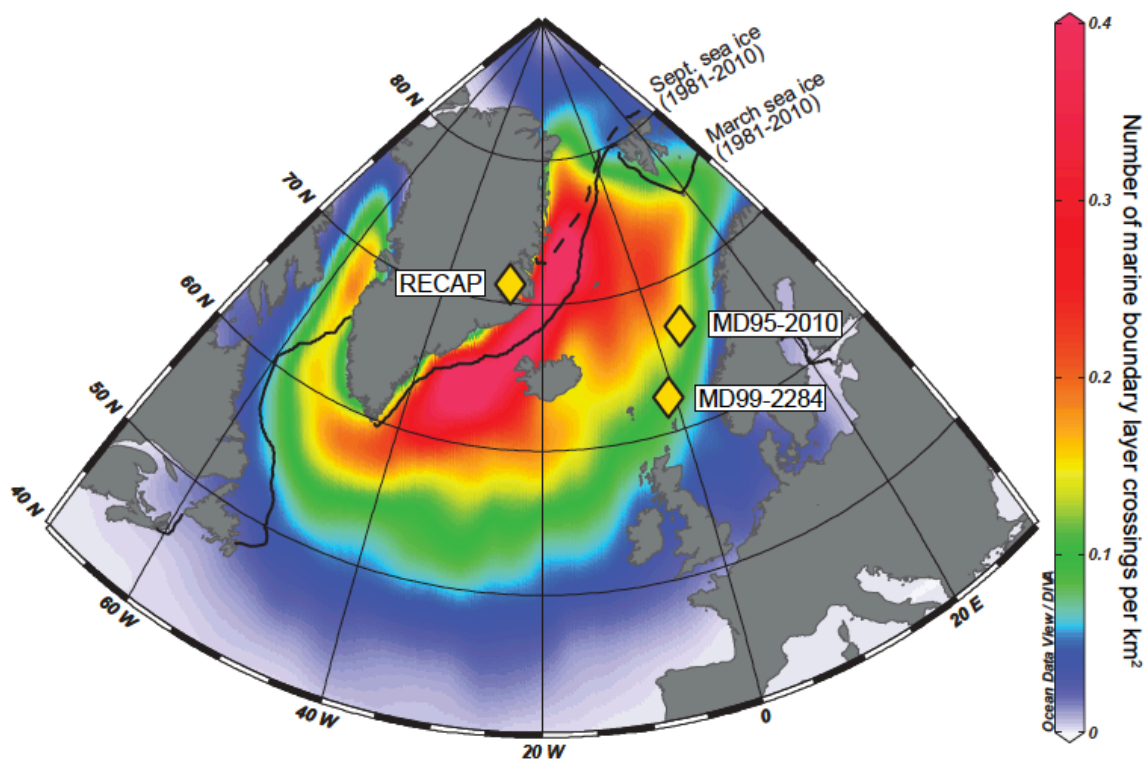


**Fig. S1.** Modern source region for bromine and sodium deposited at the RECAP ice core site. The color-coded map reflects annually averaged Marine Boundary Layer crossings per unit area ( $\text{km}^2$ ), applying a 900 hPa ( $\sim 1000$  m above sea level) constraint for at least 10 hours, based on three-day back trajectory calculations and reanalysis meteorological data for the period from 2000 to 2016 (for details see ref. 21). Regions with green, yellow and red shadings are considered as modern aerosol source region for the RECAP ice core site, including the northern North Atlantic and the Nordic Seas between  $\sim 50^\circ\text{N}$  and  $85^\circ\text{N}$  (21). Yellow diamonds mark the core sites investigated in this study. Black lines mark the modern sea ice extent during September (dashed) and March (solid), averaged between A.D. 1981 and 2010 (<http://nsidc.org>; ref. 23). The map was produced with Ocean Data View software (24).

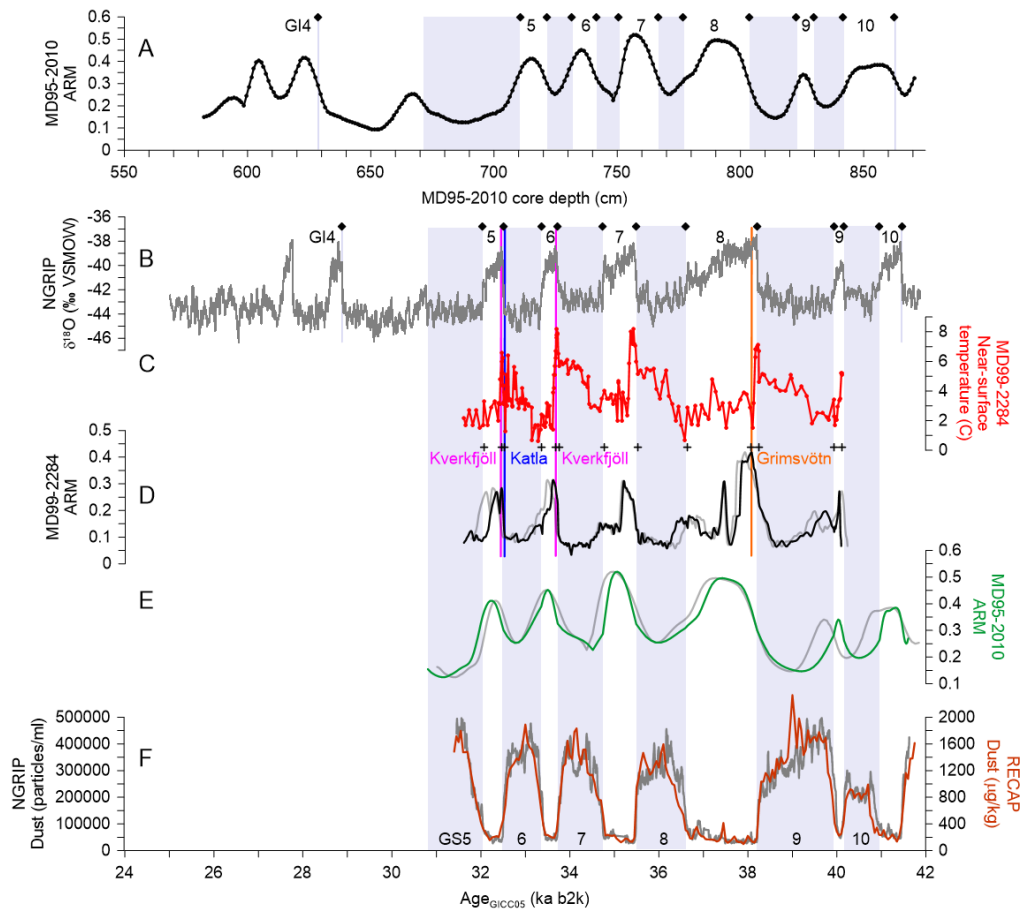


**Fig. S2.** Stratigraphic alignment and age model of the sediment and ice core records. (A) Anhyseretic remanent magnetization (ARM;  $10^{-6}$  A/m) of MD95-2010 plotted versus core depth (3, 4). (B)  $\delta^{18}\text{O}$  of the NGRIP ice core plotted as 11-point running average versus age (gray) (25). (C) Near-sea surface temperature estimates based on planktic foraminifera census counts of MD99-2284 (1) plotted versus age, based on the age model used here (2). (D) ARM ( $10^{-6}$  A/m) of MD99-2284 (1) plotted versus age, based on the age model used here (2) (black) and based on the age model by ref. 9 (gray). (E) ARM of MD95-2010 plotted versus age, based on the age model used here (green) and based on the age model by ref. 9 (gray). (F) Dust records of the RECAP ice core (10) (red) and NGRIP ice core (26) (gray). (B)-(F) are plotted on the GICC05 b2k timescale (11). Colored vertical lines in (B)-(D) mark cryptotephra layers that were identified in both MD99-2284 and the NGRIP ice core and used as isochrons based on their consistent shard geochemistry reflecting the volcanic sources (Pink, Kverkfjöll; Blue, Katla; Orange, Grímsvötn) (2). Diamonds at the top of (A) and (B) indicate stratigraphic tie points used for the age model of MD95-2010, crosses at the bottom of (C) mark tie points used for the age model of MD99-2284 (8) (Table S1; Table S2). Greenland interstadials (GI) are numbered at the top of (A) and (B), Greenland stadials (GS; shaded bars) at the bottom of (F).

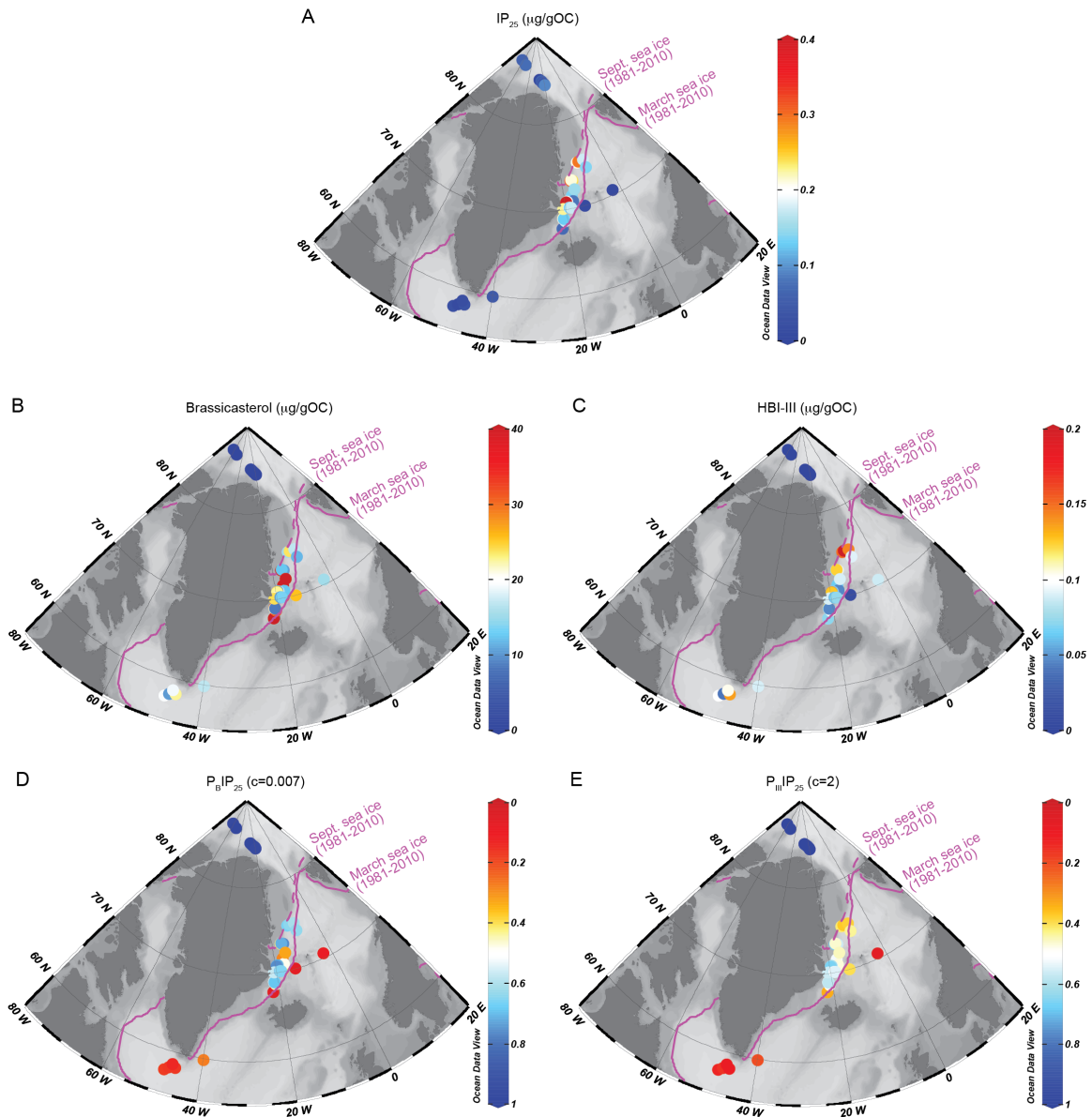


**Fig. S3.** Core-top biomarker data used in this study. Biomarker data of 41 core-tops from the north, east and south of Greenland include (A)  $IP_{25}$ , (B) Brassicasterol, (C) HBI-III, (D)  $P_BIP_{25}$  and (E)  $P_{III}IP_{25}$ . Purple lines mark the modern sea ice extent during September (dashed) and March (solid), averaged between A.D. 1981 and 2010 (<http://nsidc.org>; ref. 23). Maps were produced with Ocean Data View software (24).

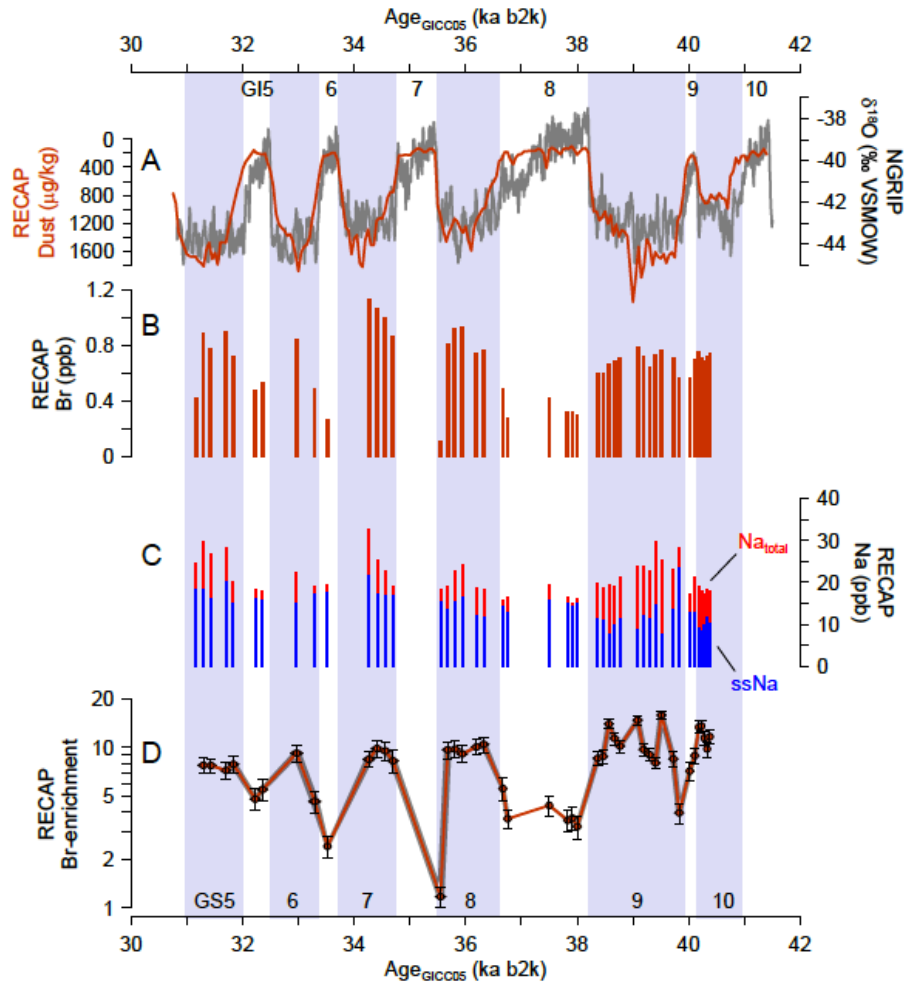


**Fig. S4.** Bromine and sodium records of the RECAP ice core. (A)  $\delta^{18}\text{O}$  of the NGRIP ice core plotted as 11-point running average (25) (gray) and dust of the RECAP ice core (10) (red). (B) Bromine values of the RECAP ice core (red). (C) Total sodium (red) and sea salt sodium (blue) of the RECAP ice core. (D) Bromine-enrichment of the RECAP ice core (red). All records are plotted on the GICC05 b2k timescale (11). Greenland interstadials (GI) are numbered at the top, Greenland stadials (GS; shaded bars) at the bottom.

**Table S1.** Age tie points, stratigraphy and sedimentation rates of core MD95-2010 for the interval ~29–41 ka. NGRIP ages are based on the GICC05 b2k chronology (11).

MD95-2010 core depth cm	NGRIP age <sub>GICC05</sub> ka b2k	Stratigraphy	Sedimentation rate cm/ka
628.50	28.885	Onset of GI4	
710.50	32.039	Termination of GI5	26.0
721.50	32.507	Onset of GI5	23.5
731.50	33.357	Termination of GI6	11.8
741.50	33.727	Onset of GI6	27.0
750.50	34.741	Termination of GI7	8.9
766.50	35.492	Onset of GI7	21.3
776.50	36.594	Termination of GI8	9.1
803.50	38.209	Onset of GI8	16.7
822.50	39.932	Termination of GI9	11.0
829.50	40.162	Onset of GI9	30.4
841.50	40.956	Termination of GI10	15.1
862.50	41.461	Onset of GI10	41.6

**Table S2.** Age tie points, stratigraphy and sedimentation rates of core MD99-2284 for the interval ~32–40 ka. We used the tie points and age model for core MD99-2284 from ref. 2. NGRIP ages are based on the GICC05 b2k chronology (11).

MD99-2284 core depth cm	NGRIP age <sub>GICC05</sub> ka b2k	Stratigraphy	Sedimentation rate cm/ka
2060.50	32.067	Termination of GI5	
2109.50	32.463	Cryptotephra layer (Kverkfjöll) during GI5	123.7
2134.50	32.522	Cryptotephra layer (Katla) during GS6	423.7
2250.50	33.363	Termination of GI6	137.9
2322.50	33.686	Cryptotephra layer (Kverkfjöll) during GI6	222.9
2355.50	33.759	Onset of GI6	452.1
2540.50	34.785	Termination of GI7	180.3
2695.50	35.526	Onset of GI7	209.2
2854.50	36.646	Termination of GI8	142.0
3038.50	38.081	Cryptotephra layer (Grímsvötn) during GI8	128.2
3085.50	38.247	Onset of GI8	283.1
3225.50	39.928	Termination of GI9	83.3
3302.50	40.108	Onset of GI9	427.8

## SI References

1. Dokken, T. M., Nisancioglu, K. H., Li, C., Battisti, D. S. & Kissel, C. Dansgaard-Oeschger cycles: Interactions between ocean and sea ice intrinsic to the Nordic seas. *Paleoceanogr. Paleoclimatology* **28**, 491–502 (2013).
2. Berben, S. M. P. *et al.* Independent tephrochronological evidence for rapid and synchronous oceanic and atmospheric temperature rises over the Greenland Stadial-Interstadial transitions between ca. 32 and 40 ka b2k. *Quat. Sci. Rev.* **236**, 106277 (2020).
3. Kissel, C. *et al.* Rapid climatic variations during marine isotopic stage 3: magnetic analysis of sediments from Nordic Seas and North Atlantic. *Earth Planet. Sci. Lett.* **171**, 489–502 (1999).
4. Dokken, T. M. & Jansen, E. Rapid changes in the mechanism of ocean convection during the last glacial period. *Nature* **401**, 458–461 (1999).
5. Sadatzki, H. *et al.* Sea ice variability in the southern Norwegian Sea during glacial Dansgaard-Oeschger climate cycles. *Sci. Adv.* **5**, eaau6174 (2019).
6. Kissel, C., Laj, C., Mulder, T., Wandres, C. & Cremer, M. The magnetic fraction: A tracer of deep water circulation in the North Atlantic. *Earth Planet. Sci. Lett.* **288**, 444–454 (2009).
7. Böhm, E. *et al.* Strong and deep Atlantic meridional overturning circulation during the last glacial cycle. *Nature* **517**, 73–76 (2015).
8. Henry, L. G. *et al.* North Atlantic ocean circulation and abrupt climate change during the last glaciation. *Science* **353**, 470–474 (2016).
9. Waelbroeck, C. *et al.* Consistently dated Atlantic sediment cores over the last 40 thousand years. *Sci. Data* **6**, 1–12 (2019).
10. Simonsen, M. F. *et al.* East Greenland ice core dust record reveals timing of Greenland ice sheet advance and retreat. *Nat. Commun.* **10**, 1–8 (2019).
11. Andersen, K. K. *et al.* The Greenland ice core chronology 2005, 15–42 ka. Part 1: constructing the time scale. *Quat. Sci. Rev.* **25**, 3246–3257 (2006).
12. Fahl, K. & Kolling, H.M. (2020): Comparison of different biomarker extraction methods, Accelerated Solvent Extractor (ASE) and ultrasonication (US), of sediment core MSM05/3\_343310-5-1. *Alfred Wegener Institute, Helmholtz Centre for Polar and Marine Research, Bremerhaven, PANGAEA*, <https://doi.org/10.1594/PANGAEA.919994>
13. Volkman, J. K. A review of sterol markers for marine and terrigenous organic matter. *Org. Geochem.* **9**, 83–99 (1986).
14. Boon, J. J. *et al.* Black Sea sterol—a molecular fossil for dinoflagellate blooms. *Nature* **277**, 125–127 (1979).
15. Belt, S. T. *et al.* A novel chemical fossil of palaeo sea ice: IP25. *Org. Geochem.* **38**, 16–27 (2007).
16. Belt, S. T., Allard, W. G., Massé, G., Robert, J.-M. & Rowland, S. J. Highly branched isoprenoids (HBIs): identification of the most common and abundant sedimentary isomers. *Geochim. Cosmochim. Acta* **64**, 3839–3851 (2000).
17. Fahl, K. & Stein, R. Modern seasonal variability and deglacial/Holocene change of central Arctic Ocean sea-ice cover: new insights from biomarker proxy records. *Earth Planet. Sci. Lett.* **351**, 123–133 (2012).

18. Müller, J. *et al.* Towards quantitative sea ice reconstructions in the northern North Atlantic: a combined biomarker and numerical modelling approach. *Earth Planet. Sci. Lett.* **306**, 137–148 (2011).
19. Xiao, X., Fahl, K., Müller, J. & Stein, R. Sea-ice distribution in the modern Arctic Ocean: biomarker records from trans-Arctic Ocean surface sediments. *Geochim. Cosmochim. Acta* **155**, 16–29 (2015).
20. Bigler, M. *et al.* Optimization of high-resolution continuous flow analysis for transient climate signals in ice cores. *Environ. Sci. Technol.* **45**, 4483–4489 (2011).
21. Maffezzoli, N. *et al.* A 120 000-year record of sea ice in the North Atlantic? *Clim. Past* **15**, 2031–2051 (2019).
22. Millero, F. J., Feistel, R., Wright, D. G. & McDougall, T. J. The composition of Standard Seawater and the definition of the Reference-Composition Salinity Scale. *Deep Sea Res. Part Oceanogr. Res. Pap.* **55**, 50–72 (2008).
23. Fetterer, F., Knowles, K., Meier, W., Savoie, M. & Windnagel, A. K. Sea Ice Index, Version 3. *NSIDC Natl. Snow Ice Data Cent.* (2017).
24. Schlitzer, R., 2018. Ocean Data View, <https://odv.awi.de>.
25. North Greenland Ice Core Project members *et al.* High-resolution record of Northern Hemisphere climate extending into the last interglacial period. *Nature* **431**, 147–151 (2004).
26. Ruth, U., Wagenbach, D., Steffensen, J. P. & Bigler, M. Continuous record of microparticle concentration and size distribution in the central Greenland NGRIP ice core during the last glacial period. *J. Geophys. Res. Atmospheres* **108**, 1–12 (2003).